Supporting Information

Experimental section

Synthesis method: In a typical procedure, MoO_3/CdS photocatalysts of variable molar ratio of MoO_3 (0, 0.1, 0.3, 0.5, 1.0 mmol MoO_3) were synthesized by sonochemical method at room-temperature and normal pressure without using any templates or surfactants. The molar ratios of MoO_3 to CdS in the composites are 1:28.5, 1:10.35, 1:6.73, 1:2.87, respectively. $Cd(Ac)_2{\cdot}2H_2O$ (3.0 mmol), $(NH_4)_6Mo_7O_{24}{\cdot}4H_2O$ (0.0143 mmol) and thioacetamide (TAA) (6.2 mmol) were dissolved in 8 mL acetone. Then the mixed solution was sonicated at ambient temperature for 1 h by a high-intensity ultrasonic probe (KQ-200KDE, Kunshan Co. China, 40 kHz) immersed directly in reaction solution. During the reaction, the temperature of the suspension was kept lower than 50 °C by refreshing the water. The precipitates were readily collected by centrifugation, washed with ethanol several times, and dried in air.

Characterization: XRD patterns were acquired on a Rigaku D/max-2000 diffractometer equipped with Cu *Kα* radiation (λ = 0.15406 nm). The morphologies of samples were performed by field emission scanning electron microscope (FESEM, FEI, Quanta 200F) and transmission electron microscopy (TEM, FEI, Tecnai G2 S-Twin). The energy-dispersive X-ray spectroscopy (EDX) implemented by FESEM was used to investigate the chemical composition of the prepared products. HAADF-STEM was carried out on a field-emission scanning transmission electron microscope, a FEI Tecnai F30, equipped with energy dispersive X-ray spectroscopy in the STEM mode. The X-ray photoelectron spectroscopy (XPS) was collected on a PHI 5700 ESCA System (USA) with an Al *Kα* chromatic X-ray source (1486.60 eV). BET specific surface area, and pore volume were calculated from nitrogen adsorption-desorption isotherms determined at 77K using an AUTOSORB-1-MP surface analyzer (the sample was outgassed under vacuum at 120 °C). UV-visible diffuse reflectance spectra were acquired by a spectrophotometer (TU-1900) and were switched from reflection to absorbance by the standard Kubelka-Munk method. The reflectance standard used $BaSO_4$. Total organic carbon (TOC) concentration in reaction was carried out on a

Shimadzu TOC-V analyzer to evaluate the mineralization of Rhodamine B (RhB). The reaction solution was investigated by Gas Chromatography-Mass Spectrometric (Agilent 6890GC-5973MS).

Photocatalytic testing: Photocatalytic activities of the samples were evaluated by H_2 production and the degradation of RhB under visible-light irradiation. The reaction was carried out by irradiating the mixture with light from a 300 W Xe lamp (λ > 400 nm). In the photocatalytic reduction for H_2 production, the photocatalyst powder was dispersed by ultrasonic for 60 min in an aqueous solution (400 mL) containing Na_2SO_3 (1.5 mol·L^{-1}) and Na_2S (0.2 mol·L^{-1}). Prior to experiment, the reaction solution was degassed with N_2. Then the photocatalytic reaction was performed in a closed gas circulation system with a side window under the N_2 atmosphere which was positioned 35 cm away from the reactor. The focused intensity on the flask was ca. 100 mW/cm^2. The amount of H_2 evolution was measured by gas chromatography (Agilent 6820) with Ar as carrier gas. The number of incident photons at 420 nm was measured by a 300 W Xe lamp with a cutoff filter and band-pass filter (λ: 420 nm, half width: 15 nm) and light flux meter (1930-C, Newport) with the light sensor. Apparent quantum yield (A.Q.Y.) was calculated by the following equation.

$$\text{A.Q.Y. (\%)} = \frac{\text{The number of reacted electrons}}{\text{The number of incident photons}} \times 100 \quad (1)$$

$$= \frac{\text{The number of evolved hydrogen molecules} \times 2}{\text{The number of incident photons}} \times 100 \quad (2)$$

In the photocatalytic reduction for pollutant photodegradation, the same 300 W Xe lamp was used as the light source, which was set about 7 cm from the liquid surface of the suspensions for RhB. The irradiation area was approximately 39cm^2. In each experiment, 0.20g of the photocatalyst was added into RhB solution (100 mL, 10 mg/L). Prior to irradiation, the suspension was first ultrasonicated for 60 min, and then magnetically stirred in the dark for 30 min to ensure adsorption equilibrium. At given time intervals, 3.5 mL suspensions were sampled, and centrifugated to remove the particles. The supernatants were analyzed at 554 nm for RhB. All the experiments were conducted at room temperature in air.

Table S1 Surface composition of synthesized MoO_3/CdS before and after reaction.

Elements	Surface atom content (%)	
	before reaction	after reaction
Cd	42.93	40.58
Mo	1.54	1.38
S	28.45	29.35
O	27.08	25.43

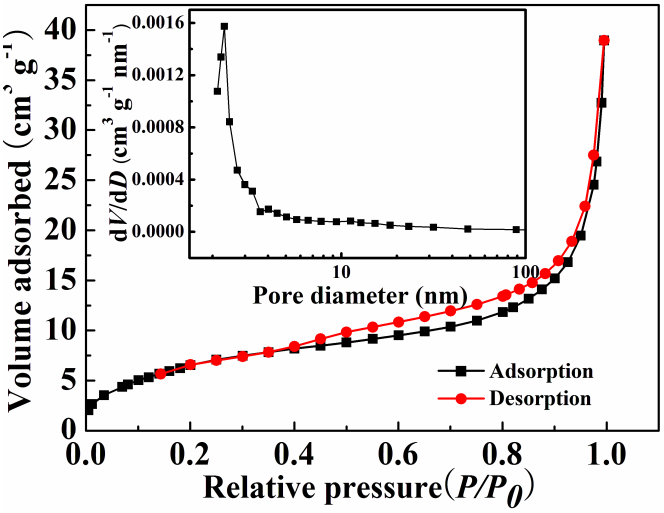

Fig. S1 N_2 adsorption-desorption isotherm and Brunauer–Emmett–Teller (BET) pore-size distribution plot of MoO_3/CdS.

As shown in **Fig. S1**, two well-defined steps at P/P_0 of 0.4-0.9 and 0.9-1.0 were observed on the N_2 adsorption-desorption isotherms. The BET surface areas of the MoO_3/CdS composites (0.1 mmol MoO_3) were 25.8231 m^2 g^{-1}, while the pore volumes were 0.062432 cm^3 g^{-1}. The sample exhibited a typical type IV with a clear H1-type hysteresis loop in the relative pressure (p/p_0) range of 0.4-0.9 which is characteristic of mesoporous materials. At high relative pressure between 0.9 and 1.0, the uptake is associated with the empty spaces between nanoparticles.[45] A pore size distribution with maximum at around 2.5 nm is also shown in the inset of **Fig. S1**. It is well-known that the larger BET specific surface areas sand the porous structure of photocatalysts can supply more surface active sites and make charge carriers transport easier for the adsorption of reactant molecules, making the photocatalytic process more efficient.[40] The larger BET specific surface areas and the unique MoO_3/CdS core/shell nanostructures containing nanopores are two important factors leading to the high photocatalytic activity under visible-light. In the photocatalytic reaction, electrons and holes generated inside the MoO_3/CdS composites can quickly migrate to the surface due to the large surface area and pore which greatly decreases the probability of recombination.[43] The mesoporous (2-50 nm) can facilitate the diffusion of reactants and products through the interior space.[40] The similar phenomenon also occurs on several other photocatalysts.[30-31]

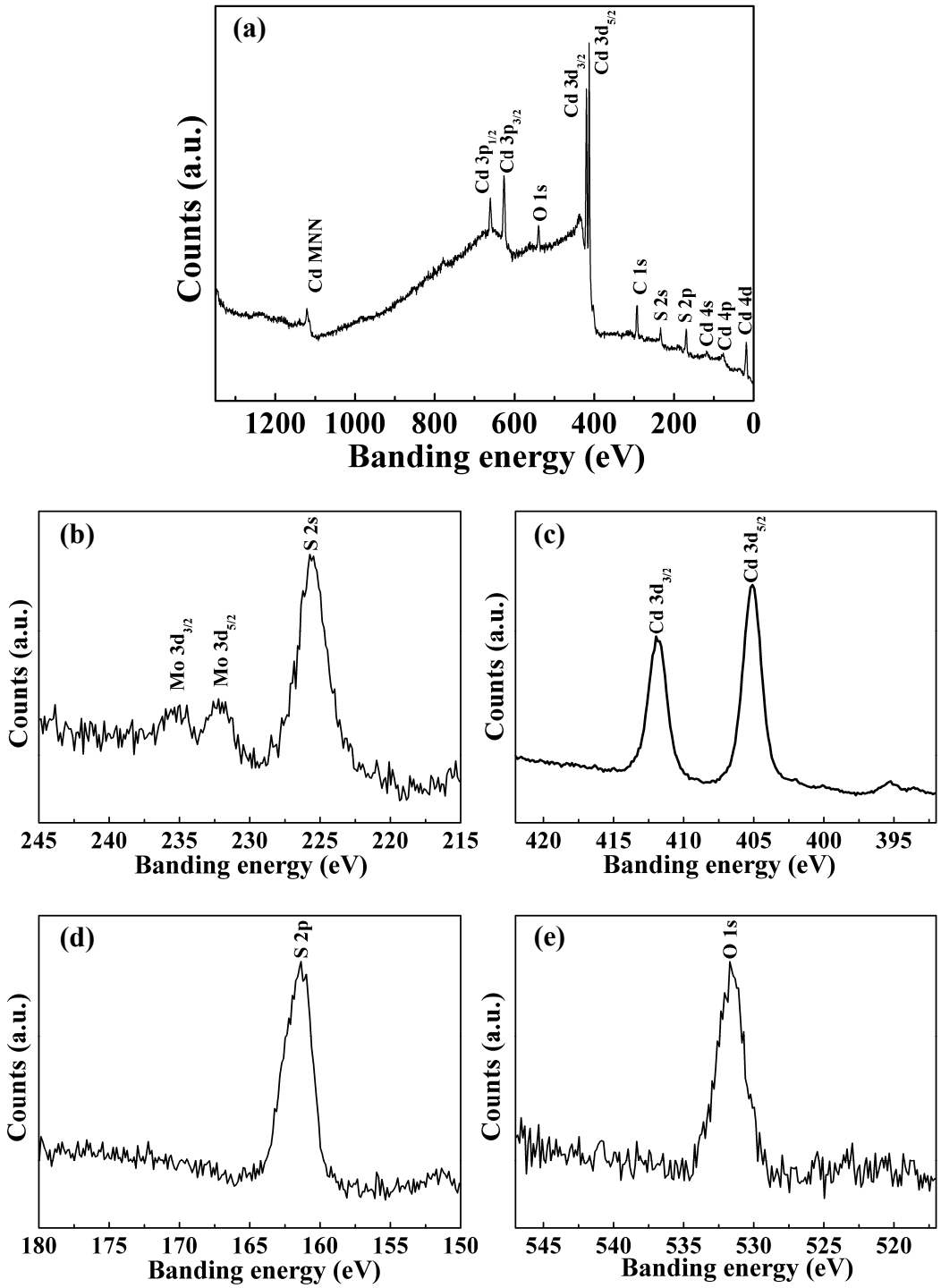

Fig. S2 XPS spectra of the sample: (a) the survey spectrum, (b) Mo 3d core level spectrum, (c) Cd 3d core level spectrum, (d) S 2p core level spectrum, (e) O 1s core level spectrum.

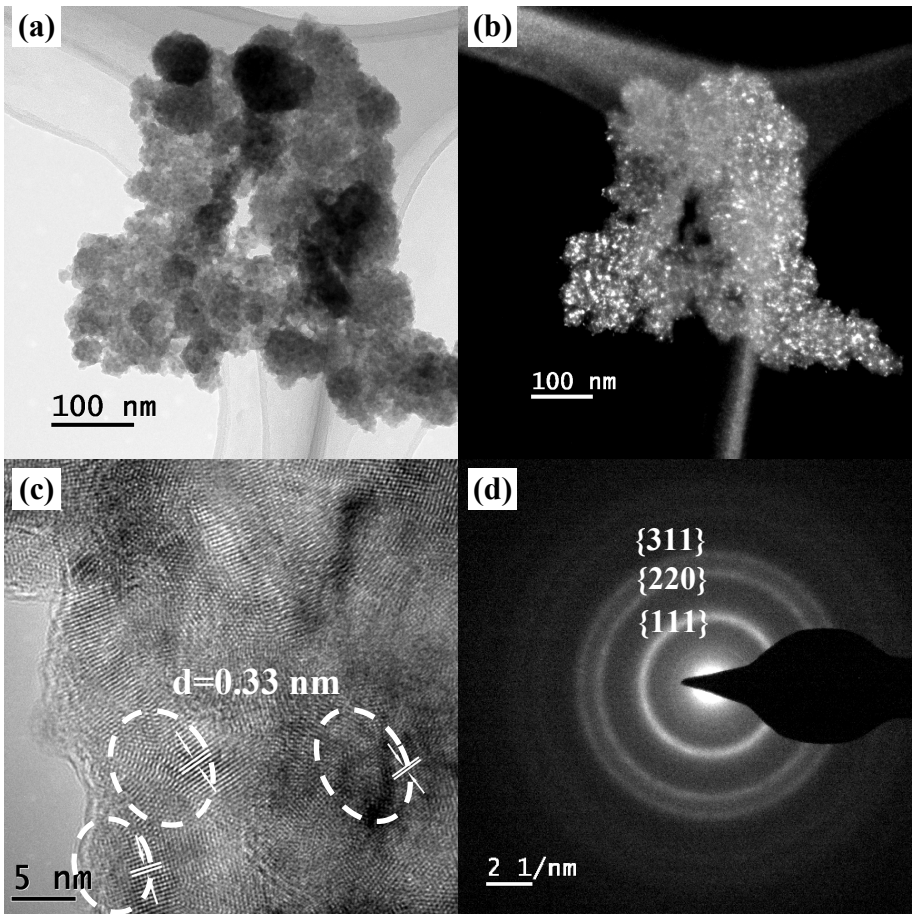

Fig. S3 TEM images of CdS nanospheres prepared by sonochemistry method: (a) TEM image, (b) DF-STEM image, (c) HRTEM image and (d) SAED pattern of sample.

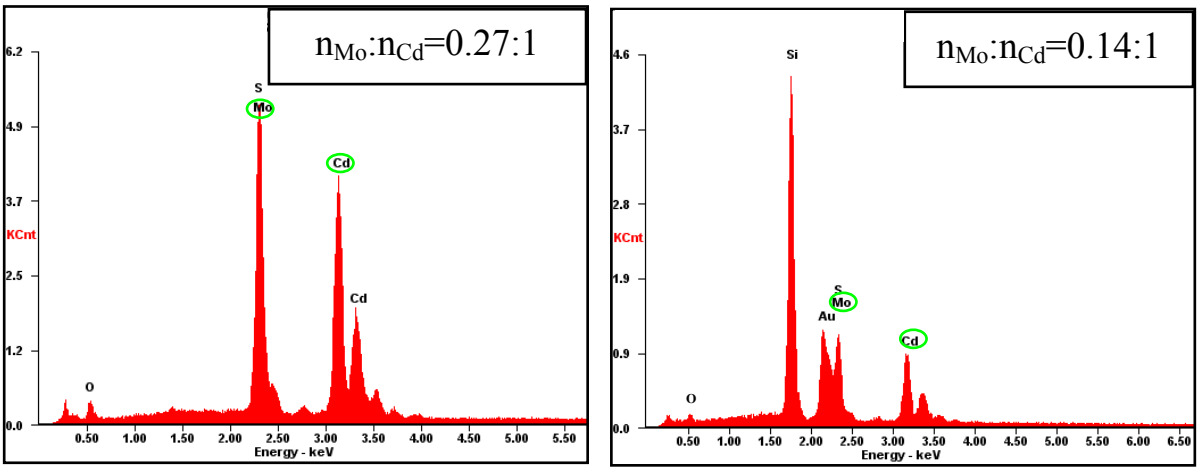

Fig. S4 EDX analysis of MoO_3/CdS samples for different reaction time: (a) 5 min, (b) 1h.

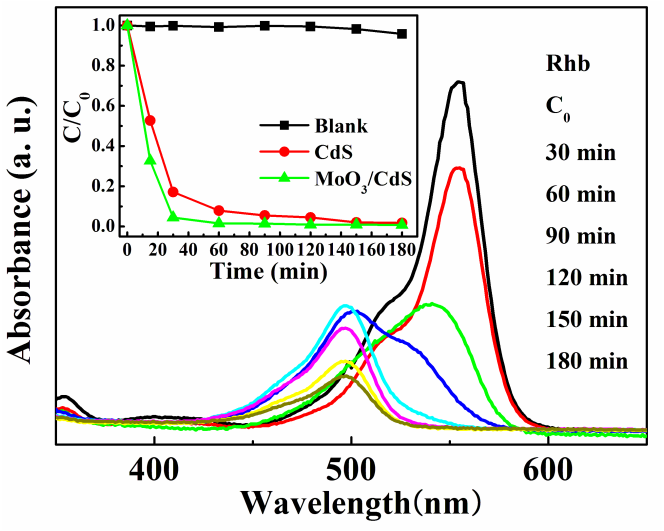

Fig. S5 UV-vis spectral changes of RhB (10 mg/L) in aqueous CdS and RhB concentration changes over blank sample, CdS and MoO_3/CdS photocatalysts.

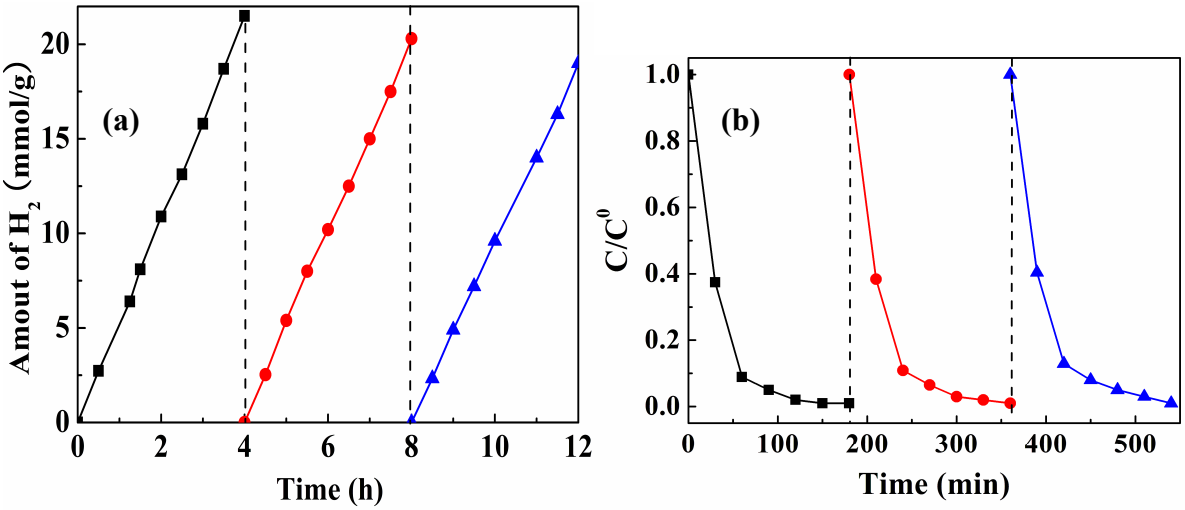

Fig. S6 (a) Amounts of H_2 evolution according to reaction time of the MoO_3/CdS photocatalysts under visible-light irradiation, (b) Cycling runs in photocatalytic degradation of RhB in the presence of the MoO_3/CdS photocatalysts under visible-light irradiation.

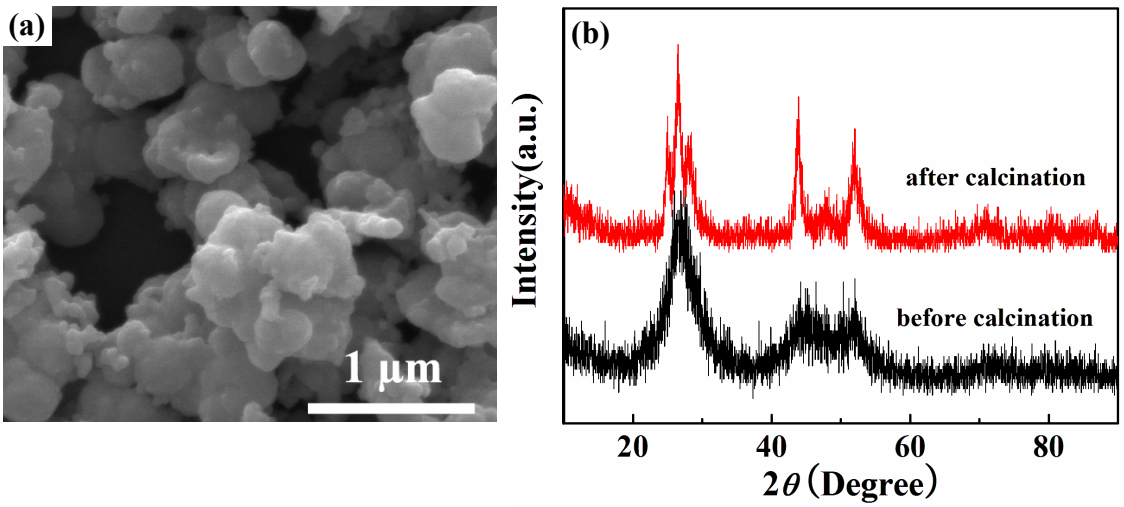

Fig. S7 (a) FESEM image of MoO_3/CdS after calcination, (b) XRD patterns of MoO_3/CdS before and after calcination.

The photocatalytic activity was evacuated after heat treatment (350°C, 1h, Ar) and the crystal structures were investigated by XRD. As shown in **Fig. S7a**, the overall morphology of MoO_3/CdS revealed the sample obvious changes after heat treatment. Although the XRD pattern showed better crystalline of sample, the rate of H_2 evolution decrease to 0.25 mmol h^{-1} g^{-1} at the initial stage which might be attributed to the disappearance of the unique nanostructures.

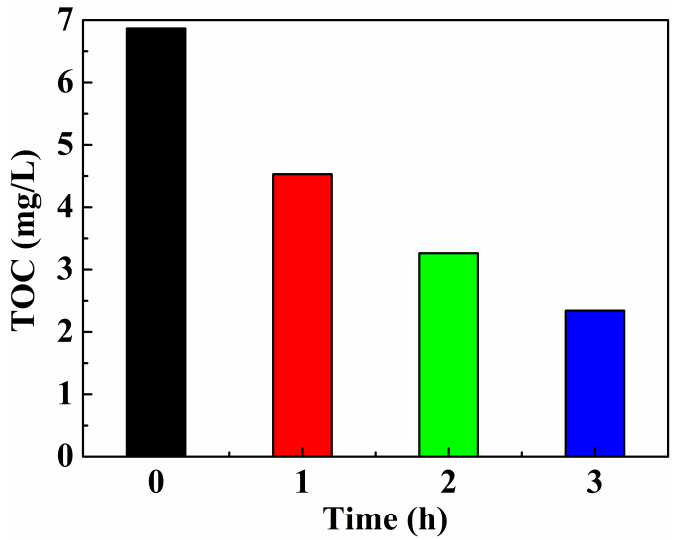

Fig. S8 Temporal decrease of total organic carbon (TOC) during the decomposition of RhB solution (initial TOC concentration, 6.86 mg/L).

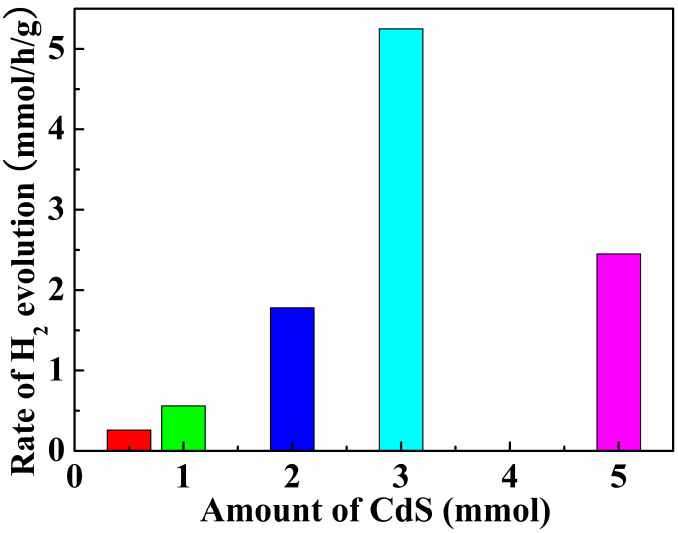

Fig. S9 Photocatalytic activities of MoO_3/CdS composites (0.5, 1, 2, 3, 5 mmol CdS)

As shown in **Fig. S9**, the rate of hydrogen evolution rapidly increases from 0.26 mmol h^{-1} g^{-1} in the presence of 0.5 mmol of CdS shell layer to the maximum rate of 5.25 mmol h^{-1} g^{-1} in the presence of 3.0 mmol of CdS shell layer and then decreases to 2.45 mmol h^{-1} g^{-1} in the presence of 5 mmol of CdS shell layer. The reason is that the amount of crystallized nanoporous CdS shell layer plays an important role on the diffusion of protons and hydrogen molecules. The crystallized small micropore (< 1 nm in diameter) in CdS shell layer deceases the fixation of large molecules, the diffusion of protons and hydrogen molecules, and in particular for the aqueous heterogeneous photocatalytic reaction involving sacrificial reagents and bulky molecules (RhB).[45] On the other hand, the majority of mesoporous (2-50 nm) in CdS shell layer can facilitate the transportation of reactants and products through the interior space due to the frameworks and interpenetrating mesoporous channels and improve the harvesting of exciting light due to enlarged surface area and multiple scattering within the porous framework.[40] In addition, with increasing shell thickness, a raised ratio in the amount of CdS to MoO_3 is attained, leading to a greater capability of light absorption for MoO_3/CdS photocatalyst and resulting in the generation of more charge carriers.[S1] Consequently, a higher number of photoexcited charge carriers are expected for MoO_3/CdS photocatalyst with larger shell thickness, which in turn promoted the resulting photocatalytic efficiency toward H_2 production and RhB photodegradation.[S1] It is worth noting that the charge

carriers' generation and transfer and the diffusion of reactants and products in crystallized nanoporous CdS shell layer are two important factors leading to the variation of MoO_3/CdS photocatalytic activity.

[S1] T. T. Yang, W. T. Chen, Y. J. Hsu, K. H. Wei, T. Y. Lin, T. W. Lin, *J. Phys. Chem. C* **2010**, *114*, 11414.

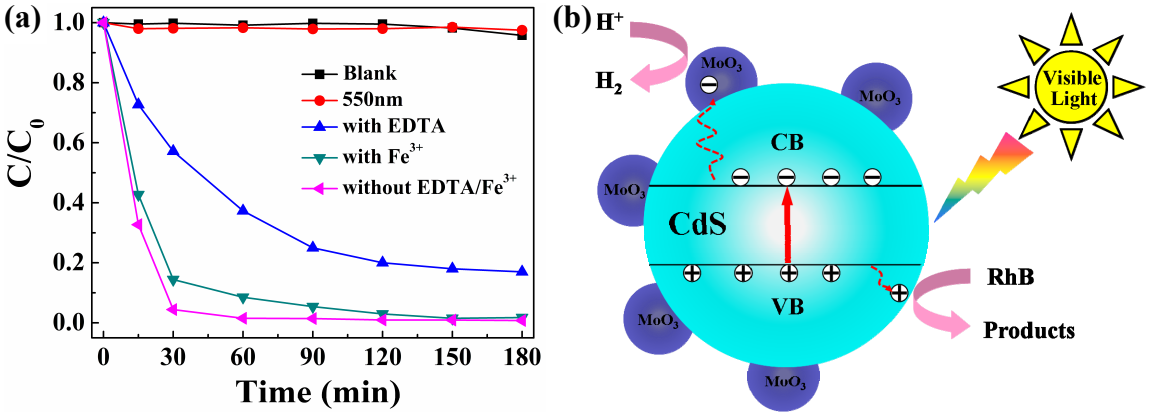

Fig. S10 (a) Photocatalytic RhB degradation over MoO_3/CdS photocatalysts without any sacrificial agent, in the presence of EDTA (10^{-3} mol L^{-1}), and in the presence of Fe^{3+} (10^{-3} mol L^{-1}). (b) Proposed mechanism for photocatalytic hydrogen production and degradation under visible light irradiation.

As shown in **Fig. 3**, there are approximately 8 major peaks that appear in the chromatogram. The GC-MS pattern in the position of 2.15 min shows the presence of acetone. The acetone serves as a suitable solvent for reaction, based on the different solubility products of the starting materials, leading to separation of product from the reaction mixture upon completion. The main organic products located at 4.0 and 8.38 min match well with the acetonitrile and acetic acid during ultrasonic reaction, respectively. Furthermore, acetonitrile could be trimerized to obtain 2,4,6-trimethyl-1,3,5-triazine with increasing the reaction time. The peaks at 7.25, 10.30, and 11.05 min can be assigned to thioacetamide's reaction by-products, corresponding to 2,5-dimethyl-1,3,4-thiadiazole, acetamide and diacetamide, respectively. Based on the analysis above, the formation and explanation of the thioacetamide's reaction by-products are listed as following:

$$CH_3CSNH_2 \xrightarrow[C_3H_6O/air]{)))} CH_3CN + H_2S \quad (3)$$

$$3CH_3CN \xrightarrow[C_3H_6O/air]{)))} \quad (4)$$

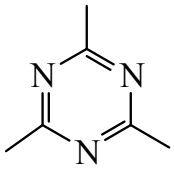

$$CH_3CSNH_2 + H_2O \xrightarrow[C_3H_6O/air]{)))} CH_3CONH_2 + H_2S \quad (5)$$

$$2CH_3CONH_2 \xrightarrow[C_3H_6O/air]{)))} H_3C-\overset{\overset{O}{\|}}{C}-NH-\overset{\overset{O}{\|}}{C}-CH_3 + NH_3 \quad (6)$$

$$2CH_3CSNH_2 \xrightarrow[C_3H_6O/air]{)))} \left[H_3C-\overset{\overset{S}{\|}}{C}-NH-NH-\overset{\overset{S}{\|}}{C}-CH_3 \right] \xrightarrow[C_3H_6O/air]{)))}$$

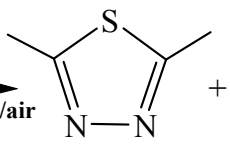

$+ H_2S(5)$